e-*Blood*

The biology of nematode- and IL4Rα-dependent murine macrophage polarization in vivo as defined by RNA-Seq and targeted lipidomics

Graham D. Thomas,[1] Dominik Rückerl,[1] Benjamin H. Maskrey,[2] Phillip D. Whitfield,[2] Mark L. Blaxter,[1] and Judith E. Allen[1]

[1]Institute of Immunology and Infection Research and Institute of Evolutionary Biology, School of Biological Sciences, University of Edinburgh, Edinburgh, United Kingdom; and [2]Lipidomics Research Facility, Department of Diabetes and Cardiovascular Science, University of the Highlands and Islands, Inverness, United Kingdom

Alternatively activated macrophages (AAMϕ) are a major component of the response to helminth infection; however, their functions remain poorly defined. To better understand the helminth-induced AAMϕ phenotype, we performed a systems-level analysis of in vivo derived AAMϕ using an established mouse model. With next-generation RNA sequencing, we characterized the transcriptomes of peritoneal macrophages from BALB/c and IL4Rα$^{-/-}$ mice elicited by the nematode *Brugia malayi*, or via intraperitoneal thioglycollate injection. We defined expression profiles of AAMϕ-associated cytokines, chemokines, and their receptors, providing evidence that AAMϕ contribute toward recruitment and maintenance of eosinophilia. Pathway analysis highlighted complement as a potential AAMϕ-effector function. Up-regulated mitochondrial genes support in vitro evidence associating mitochondrial metabolism with alternative activation. We mapped macrophage transcription start sites, defining over-represented *cis*-regulatory motifs within AAMϕ-associated promoters. These included the binding site for PPAR transcription factors, which maintain mitochondrial metabolism. Surprisingly PPARγ, implicated in the maintenance of AAMϕ, was down-regulated on infection. PPARδ expression, however, was maintained. To explain how PPAR-mediated transcriptional activation could be maintained, we used lipidomics to quantify AAMϕ-derived eicosanoids, potential PPAR ligands. We identified the PPARδ ligand PGI_2 as the most abundant AAMϕ-derived eicosanoid and propose a PGI_2-PPARδ axis maintains AAMϕ during *B malayi* implantation. (*Blood*. 2012; 120(25):e93-e104)

Introduction

Macrophages display enormous functional diversity determined by signals from their immediate environment. IFNγ stimulation induces classic activation, an essential prerequisite for microbial infection control, whereas IL4/IL13 exposure polarizes macrophages toward alternative activation.[1] Alternatively activated macrophages (AAMϕ) are now implicated in the promotion of a wide range of diseases, including cancer,[2] allergy,[1] and fibrosis,[1] but also in protection against helminth infection,[3] diabetes,[4] and obesity.[4]

Despite the flurry of interest in AAMϕ, we remain remarkably ignorant of their physiologic role(s), partly because classic and alternative activation represents polar regions in a landscape of activation phenotypes sculpted by multiple factors. Different cellular developmental histories,[5] microenvironmental cues, and factor-dependent polarization[6] vastly increase the complexity of macrophage phenotypes in vivo. IL4/IL13 induce canonical alternative activation via IL4Rα-dependent phosphorylation of STAT6, driving the transcription of a diverse repertoire of genes, including *Arg1* (Arginase-1), *Chi3l3* (Chitinase 3-like 3, YM-1), and *Retnla* (resistin-like α, RELMα, FIZZ-1). Because exposure to helminths almost universally induces potent Th2 responses, alternative activation of Mϕ is characteristic of these infections.[7] Indeed, *Chi3l3* and *Retnla* were described as AAMϕ markers associated with challenge by the parasitic nematode *Brugia malayi*.[7]

An emerging paradigm suggests that cytokine-mediated alterations in cellular metabolism determine cellular life-history[8] and effector functions.[9] For example, a switch from glucose dependency to mitochondrial metabolism oversees the ability of effector $CD8^+$ T cells to commit to a memory phenotype.[8] In this context, it is interesting to note that in vitro studies suggest that classically activated macrophages (CAMϕ) and AAMϕ are associated with different metabolic profiles. CAMϕ require aerobic glycolysis,[10] whereas AAMϕ couple lipid oxidation with oxidative phosphorylation.[4] Cooperative interactions between STAT6, PPARγ, and PGC-1β are considered necessary[4,11] to induce these metabolic changes in AAMϕ. In vivo confirmation of this observation is required, and an improved understanding of the role for mitochondrial metabolism in alternative activation may yield key insights into the effector functions of these cells.

Previous transcriptome analyses of AAMϕ have used in vitro-generated cells, whereas in vivo studies of Th2 environments have analyzed whole tissue.[12,13] This leaves a gap in our understanding of AAMϕ function during infection. Previously, we identified abundantly expressed genes in in vivo–derived AAMϕ using an expressed sequence tag approach.[7] This provided valuable insight into markers expressed by these cells but lacked the power to critically assess molecular pathways associated with alternative

Submitted July 11, 2012; accepted October 10, 2012. Prepublished online as *Blood* First Edition paper, October 16, 2012; DOI 10.1182/blood-2012-07-442640.

This article contains a data supplement.

The publication costs of this article were defrayed in part by page charge payment. Therefore, and solely to indicate this fact, this article is hereby marked "advertisement" in accordance with 18 USC section 1734.

activation in vivo. Here, using second-generation Illumina sequencing and mass spectrometry, we combined transcriptomics and lipidomics to gain a global overview of macrophage IL4Rα-dependent transcription and transcriptional regulation in vivo.

We compared nematode-elicited macrophages (NeMϕ) and inflammatory-like thioglycollate-elicited macrophages (ThioMϕ) from both wild-type (WT) and IL4Rα$^{-/-}$ mice. We sought to define physiologic functions of in vivo–derived AAMϕ and have focused on understanding the macrophage response to filarial nematode infection. We defined macrophages as F4/80-positive cells with a negative gating strategy to exclude contaminants. This definition probably includes macrophage subpopulations that contribute differentially toward the overall response; however, this comparison allowed us to focus on the most relevant changes in macrophage physiology to filarial nematode challenge. The contrast between WT-NeMϕ and WT-ThioMϕ identified differential gene expression due to the presence of the nematode, or differences in cell origin. Comparing WT-NeMϕ and IL4Rα$^{-/-}$-NeMϕ revealed IL4Rα-dependent components of macrophage activation during helminth infection. We followed Siamon Gordon's definition of alternative activation as the IL4/IL13–dependent component of macrophage activation.[1] IL4Rα deficiency ablates both IL4– and IL13–dependent signaling.[1] Thus, coordinately differentially expressed (DE) genes in WT-NeMϕ (ie, in vivo generated AAMϕ) relative to both WT-ThioMϕ and IL4Rα$^{-/-}$-NeMϕ are, by definition, those relevant to alternative activation during helminth infection.

Illumina RNA sequencing (RNA-Seq) provided $>$ 5 orders of magnitude dynamic range between the most abundant and lowly expressed genes, delivering the most extensive characterization of in vivo–polarized macrophage populations to date. We establish a putative role for AAMϕ in eosinophil recruitment and the complement response during helminth infection. Macrophage transcription start sites (TSSs) were mapped; and, by characterizing over-represented *cis*-regulatory elements in AAMϕ promoters, we confirm PPAR-dependent transcription as a major facilitator of alternative activation in vivo. Pathway analysis supported these findings by identifying AAMϕ-dependent alterations in lipid and mitochondrial metabolism, key targets of PPAR transcription factors. Finally, liquid chromatography-tandem mass spectrometry (LC-MS/MS) was used to define the *B malayi*–induced repertoire of endogenous eicosanoids, allowing us to propose a mechanism for PPARδ-mediated alternative activation. We thus provide global mechanistic insights into the function and regulation of helminth-elicited AAMϕ and identify putative effector molecules involved in the maintenance and regulation of alternative activation in vivo.

Methods

Generation of macrophage populations

Nine WT BALB/c and 9 IL4Rα$^{-/-}$ mice were infected with 4 *B malayi* adult females and 1 male by surgical implant, or challenged with an intraperitoneal thioglycollate injection (700 μL of 4% Brewer-modified thioglycollate medium in PBS [weight/volume], BD Biosciences Pharmingen) as described previously.[5] All work was conducted in accordance with the Animals (Scientific Procedures) Act of 1986. *B malayi* were obtained from Mongolian jirds purchased from TRS Laboratories. Twenty-one days after implantation, or 3 days after thioglycollate treatment, whole peritoneal exudate cells (PECs) were extracted by lavage with RPMI + HEPES, 1% penicillin/streptomycin, 2mM EDTA, and macrophages purified by FACS.

FACS purification and intracellular cytokine staining

PECs were treated with red blood cell lysis media (Sigma-Aldrich) and up to 1×10^7 cells retained per mouse for FACS sorting. PEC cells were stained with Live/Dead Aqua (Invitrogen), F4/80-biotin (BioLegend), SiglecF-PE, B220-PE, CD4-FITC, and streptavidin-allophycocyanin (eBioscience) before sorting on a FACSAria (BD Biosciences). F4/80$^+$ macrophages were sorted based on allophycocyanin positivity. Negative gating based on PE and FITC staining was used to ensure the highest possible purity (Figure 1; supplemental Figure 1, see the Supplemental Materials link at the top of the article). Macrophage purity was verified by flow cytometry and stored in Qiazol (QIAGEN) before RNA extraction. Alternative activation in WT-infected mice was confirmed using intracellular staining for RELMα as described previously.[5]

RNA-Seq library preparations, high-throughput sequencing, and bioinformatic analyses

Full details are provided in the supplemental Methods. Briefly, RNA was extracted using the QIAGEN miRNeasy kit and quality assessed on an Agilent Bioanalyzer. RNA-Seq libraries were prepared from 2 μg of RNA, each obtained by pooling 0.66 μg from 3 mice, using the Illumina paired-end RNA-Seq library preparation kit. Fifty-one base paired-end RNA-Seq libraries were sequenced on an Illumina GAIIx, and reads were mapped to the mouse reference genome using TopHat. Differential expression analysis was performed using DESeq, and TSSs predicted using the custom algorithm TSS-Predictor. Gene set enrichment and hierarchical cluster analysis were performed in the R environment.

Lipidomics

Full details of the lipidomic experimental methods are given in supplemental Methods. Briefly, in an independent homologous experiment to the RNA-Seq, adherence purified macrophages from whole PECs were cultured for 12 hours. Total eicosanoids were extracted from peritoneal lavage supernatant and purified macrophage cultures using C18 solid phase extraction cartridges, after spiking with known amounts of the deuterated internal standards 15-hydroxyeicosatetraenoic acid (15-HETE)-d8, LTB_4-d4, and PGE_2-d4. Eicosanoids were separated on a Thermo Scientific Hypersil Gold C18 column (3 μm × 2.1 × 50 mm) directed into an online tandem mass spectrometer (TSQ Quantum Ultra; Thermo Scientific) operating in negative ion mode. Data were acquired and analyzed using LCquan Version 2.6 software (Thermo Scientific).

Results

Generation of AAMϕ and differential expression analysis

We generated NeMϕ and ThioMϕ by implanting BALB/c and IL4Rα$^{-/-}$ mice with the nematode *B malayi,* or via intraperitoneal administration of thioglycollate to elicit a population of nonpolarized, inflammatory-like macrophages. IL4 stimulation increases F4/80 surface expression on macrophages.[5] To enrich for AAMϕ in the implant setting, we collected the brightest F4/80$^+$ macrophage population in each condition (supplemental Figure 1). Macrophage purity was maximized by exclusion of dead cells, doublets, B cells (B220$^+$), eosinophils (SiglecF$^+$), and CD4$^+$ T cells using negative gating (Figure 1A). Our sorting strategy resulted in an average of 97.3% purity (range, 94.9%-99.4%, supplemental Table 1). Alternative activation of WT-NeMϕ was confirmed with intracellular cytokine staining for RELMα (Figure 1B-C). On average, 47% of WT-NeMϕ were RELMα positive, consistent with 30%-60% positivity typically seen after *B malayi* implant. RNA-Seq libraries yielded between 11 million and 30 million 51-base

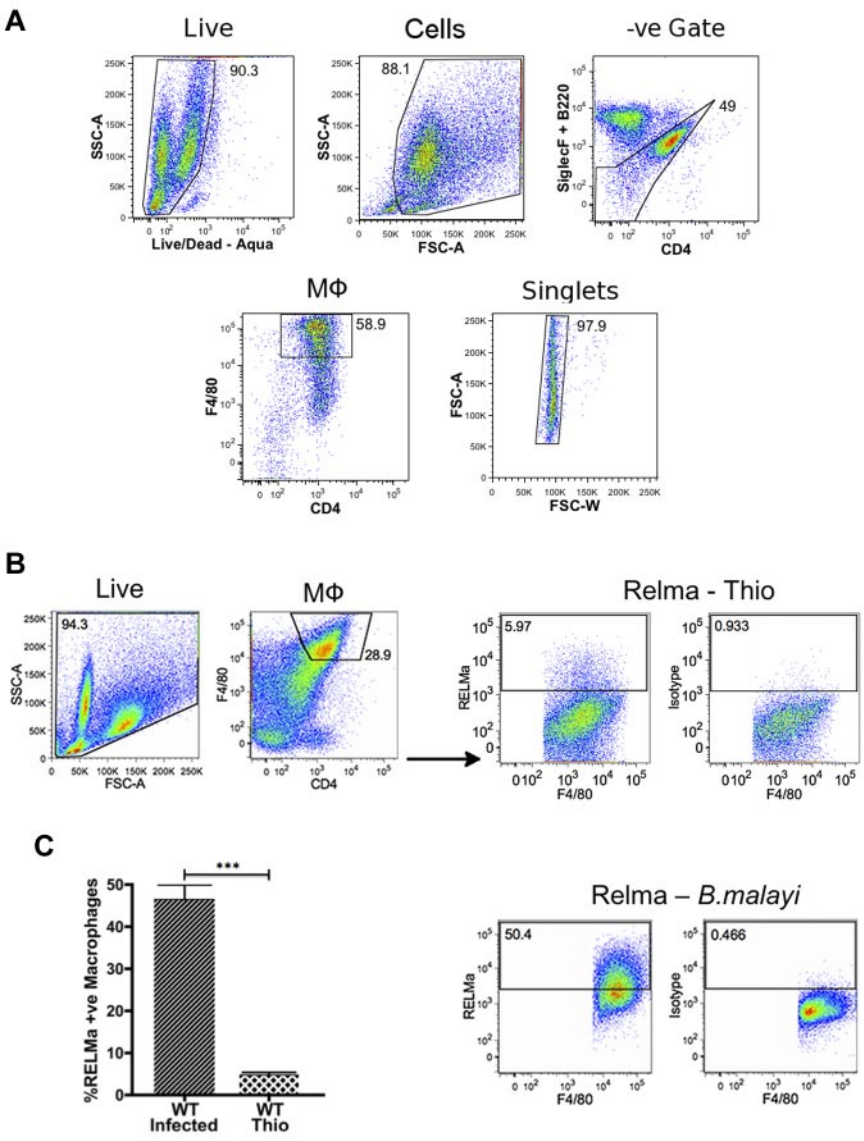

Figure 1. Flow cytometric acquisition of macrophages and confirmation of alternative activation in WT *B malayi*–implanted macrophages. (A) Gating strategy used to obtain pure macrophage populations as shown with 1 representative WT *B malayi*–infected individual. After the removal of dead cells, B220, SiglecF, and CD4-positive cells were excluded. F4/80 high cells were then selected and doublets removed based on forward scatter width (FSC-W)/forward scatter area (FSC-A). (B) Intracellular cytokine staining for RELMα expression in thioglycollate-elicited macrophages (top) and *B malayi*–elicited macrophages (bottom). The scatter profile and macrophage gates on the left refer to 1 representative WT *B malayi*–infected individual. (C) Bar chart showing percentage of RELMα-positive macrophages from analysis. (B) n = 9 per group. ***$P < .001$.

paired-end reads. Gene expression was quantified by mapping reads to the mouse reference genome using TopHat.[14] In total 55%-73% of reads mapped uniquely to the genome, with 7.7-25 million mapping within exons of known genes (Ensembl Version 58, Table 1). Between 12 853 and 13 520 (56%-59%) protein coding genes were expressed in each group, with 12 039 of these common to all 4 populations (Figure 2A). We validated sample purity by assessing the expression of lineage-restricted

Table 1. Sequence and mapping statistics for raw Illumina data

Strain	Treatment	Repeat	Total reads	No. mapped	% mapped	Properly paired	% properly paired	Singletons	% singletons	Unique reads in ensembl v58 annotations	% unique reads in ensembl v58 annotations
BALB/c	Infected	1	35 646 760	24 026 742	67.4	18 883 064	78.59	3 802 882	15.83	13 914 673	57.9
BALB/c	Infected	2	39 663 694	26 450 844	73.3	21 349 672	80.71	4 071 578	15.39	15 261 028	57.7
BALB/c	Infected	3	40 960 176	26 670 826	65.1	20 637 676	77.38	4 486 602	16.82	15 578 573	58.4
BALB/c	Thio	1	40 398 232	26 011 652	64.3	21 817 520	83.88	3 454 426	13.28	14 732 920	56.6
BALB/c	Thio	2	48 366 774	33 194 643	68.6	26 782 502	80.68	5 494 173	16.55	19 344 275	58.2
BALB/c	Thio	3	45 552 296	28 796 129	63.2	24 350 132	84.56	4 167 411	14.47	16 480 896	57.2
IL4Rα$^{-/-}$	Infected	1	56 700 552	31 428 896	55.4	27 125 044	86.31	4 172 298	13.28	17 799 754	56.6
IL4Rα$^{-/-}$	Infected	2	23 150 358	15 076 797	65.1	12 977 824	86.08	1 911 075	12.68	8 493 659	56.3
IL4Rα$^{-/-}$	Infected	3	60 376 960	42 872 365	71.0	32 888 162	76.71	6 826 787	15.92	24 849 426	57.9
IL4Rα$^{-/-}$	Thio	1	40 492 838	24 144 541	59.6	19 772 782	81.89	3 547 653	14.69	13 845 966	57.3
IL4Rα$^{-/-}$	Thio	2	22 996 482	13 033 134	56.7	8 952 742	68.69	2 418 168	18.55	7 725 619	59.2
IL4Rα$^{-/-}$	Thio	3	36 062 844	19 911 073	55.2	14 751 228	74.09	3 874 775	19.46	11 892 859	59.7

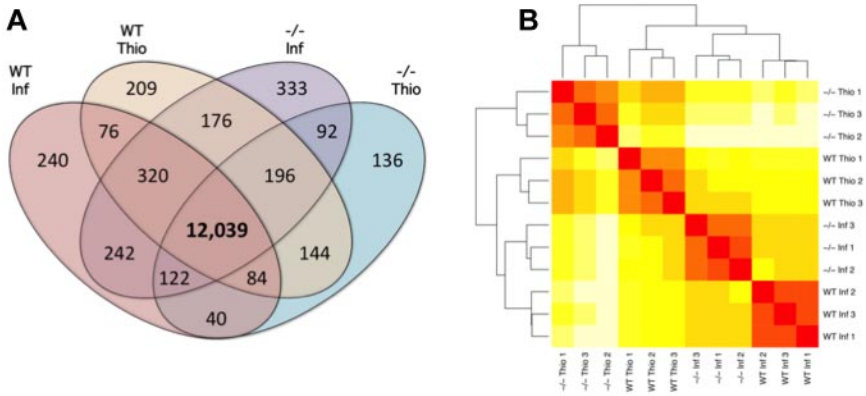

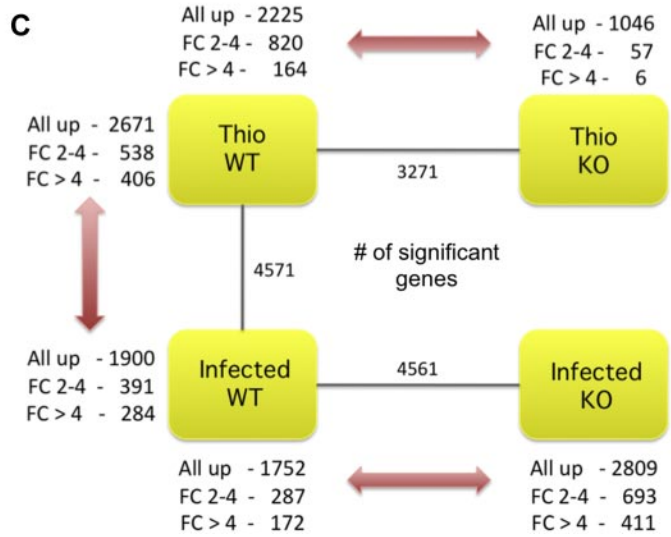

Figure 2. Overall gene expression and differential expression analysis. (A) Number of expressed genes in macrophage populations where expressed is considered as at least 1 read mapping to a gene in all 3 replicates of a condition. (B) Unsupervised, hierarchical clustering of individual lanes demonstrating discrete clustering of biologic replicates. (C) Summary of DE genes ($P < .01$) in each pairwise comparison showing the total number of DE genes (inner), and a breakdown showing the direction of differential expression for both moderately (log 2-fold change ± 2-4) and highly (log 2-fold change > 4) DE genes.

marker genes for potential contaminants; eosinophils, neutrophils, and B cells (supplemental Table 2). With this approach, we confirmed negligible contamination of neutrophils or eosinophils; however, a low level of *Cd19* expression was observed in IL4Rα$^{-/-}$-NeMϕ.

Hierarchical clustering of global gene expression profiles grouped RNA-Seq libraries according to biologic condition, reaffirming the quality and reproducibility of our analysis (Figure 2B). After differential expression analysis, we identified substantial transcriptional differences between the macrophage populations in the 3 key comparisons (Figure 2C). Using a *P* value cutoff of .01 after correction for multiple testing (Benjamini-Hochberg method), we identified 4571 DE genes between WT-NeMϕ and WT-ThioMϕ, 4561 DE genes between WT-NeMϕ and IL4Rα$^{-/-}$-NeMϕ, and 3271 DE genes between WT-ThioMϕ and IL4Rα$^{-/-}$-ThioMϕ (Figure 2C). A complete gene list and associated *P* values are provided in supplemental Table 3. We observed a higher number of DE genes between WT-NeMϕ and IL4Rα$^{-/-}$-NeMϕ than between WT- ThioMϕ and IL4Rα$^{-/-}$-ThioMϕ (Figure 2C). In addition, the magnitudes of these differences were much greater in the infection setting (supplemental Figure 7). Furthermore, a similar range of differential expression was observed between WT-NeMϕ and WT-ThioMϕ as for WT-NeMϕ and IL4Rα$^{-/-}$-NeMϕ. Thus, as expected, IL4Rα-dependent signaling drove major alterations in the macrophage transcriptional profile in response to Th2-inducing immune stimuli.

We interrogated the expression profiles of DE genes to identify those explicitly associated with alternative activation. All DE genes from the WT-NeMϕ versus WT-ThioMϕ and WT-NeMϕ versus IL4Rα$^{-/-}$-NeMϕ comparisons (4571 and 4561, respectively) were grouped according to their expression profile using hierarchical agglomerative clustering. The resulting tree was subdivided into 20 clusters, and the expression profile of genes in each cluster was assessed (supplemental Figure 8). We identified 5 clusters with increased expression levels in WT-NeMϕ relative to both WT-ThioMϕ and IL4Rα$^{-/-}$-NeMϕ. These were classified as AAMϕ-up (Figure 3; supplemental Table 4). Similarly, 5 clusters were identified with converse expression profiles and classified as AAMϕ-down. In total, 1658 genes AAMϕ-up genes and 1735 AAMϕ-down genes were identified (Figure 3). Importantly, we can state that expression of genes in AAMϕ-up and AAMϕ-down clusters is IL4Rα-dependent. However, as the IL4Rα$^{-/-}$ mice lack IL4Rα expression on all cells, we cannot say whether these effects are cell-autonomous and, in some cases, may reflect other changes, such as Th2 cell activation.

Differential expression of immune effectors

We reasoned that a descriptive, knowledge-based, assessment of immunologically relevant GO terms (encompassing cytokines, chemokines, and their receptors; GO terms GO:0005125, GO:0008009, GO:0004896, and GO:0004950, respectively; hereafter called immune effectors) would provide insight into AAMϕ function and regulation. Immune effectors that were present in AAMϕ-up and AAMϕ-down clusters were defined as AAMϕ-associated. Using this criterion, we identified AAMϕ-association

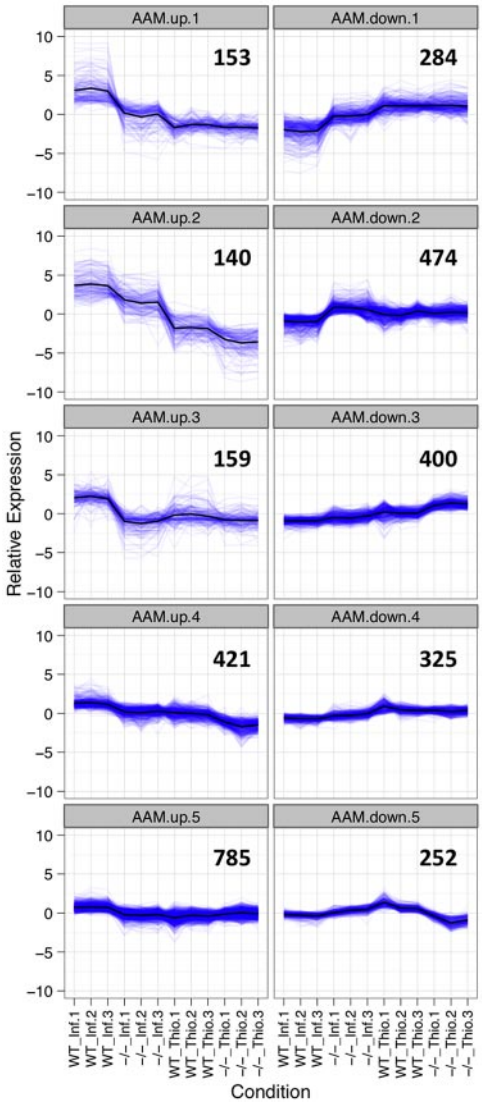

Figure 3. Expression profiles of differentially expressed AAMϕ-associated gene sets. The expression profiles of gene sets positively and negatively associated with alternative activation (AAMϕ-up and AAMϕ-down). All statistically significant genes ($P < .01$) between WT-NeMϕ and WT-ThioMϕ, and WT-NeMϕ and IL4Rα$^{-/-}$-NeMϕ, were clustered using hierarchical agglomerative clustering. Each gene within an expression cluster is plotted in blue, and the mean expression for all genes within each cluster is overlaid in black. The figure in each panel represents the total number of genes in that cluster.

for 16 cytokines, 11 cytokine receptors, 10 chemokines, and 8 chemokine receptors (Figure 4). Here we discuss the function of key AAMϕ-associated immune effectors, providing insight into the IL4Rα-dependent facets of the macrophage response to filarial nematode infection in vivo and defining candidate genes for future investigations.

Chemokine and chemokine receptor expression profiles. The AAMϕ chemokine expression profile (Figure 4) was consistent with macrophage-mediated maintenance of the cellular milieu in the peritoneal cavity of *B malayi*–implanted mice, which is composed primarily of B cells, macrophages, and eosinophils.[15] All assayed macrophage populations abundantly and constitutively expressed *Ccl6* and *Ccl9* (supplemental Table 5), which may serve to maintain macrophage populations within the peritoneal cavity.[16] In the AAMϕ-up clusters, we identified the eosinophil chemoattractants *Ccl24* and *Ccl8*,[16] as abundantly and moderately expressed, respectively. *Cxcl12* and *Cxcl13* were also identified as AAMϕ-associated, however, were expressed at much lower levels. Consistent with an anti-inflammatory or noninflammatory phenotype of AAMϕ,[1] the AAMϕ-down clusters contained *Ccl3* (Mip1α), *Ccl4*, *Ccl2* (MCP-1), *Ccl7* (MCP-3), and *Cxcl14*, all of which are involved in acute phase inflammation, attracting primarily monocytes and neutrophils.[17]

Interestingly, AAMϕ-up clusters were devoid of chemokine receptors with the exception of *Cxcr7* (Figure 4). Cxcr7 responds to the stromal-derived Cxcl12, affecting both migration and differentiation in monocytes.[18] *Ccr1* (MIP-1α receptor, supplemental Table 5) was also highly expressed by macrophages, but not classified as AAMϕ-associated. Therefore, *Cxcr7* and/or *Ccr1* may be key determinants of nematode-induced AAMϕ localization.[17,18] A large number of chemokine receptors were present in the AAMϕ-down clusters. These included *Ccr2*, *Cxcr1*, *Cxcr2*, *Cxcr3*, *Ccr5*, and *Ccrl2*, implying that AAMϕ are impaired in their capacity to respond to numerous chemokines. This suggests that WT-NeMϕ do not migrate to prime lymphatic T-cell responses, despite high MHCII expression and functional antigen presentation.[19,20]

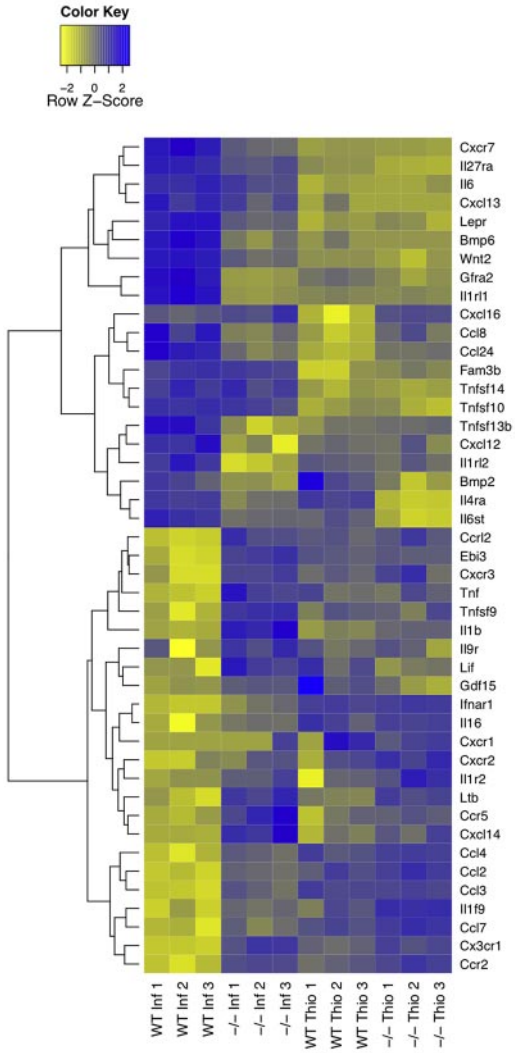

Figure 4. Heatmap of alternative activation-modulated immune effectors. Immune effector genes, cytokines, chemokines, and their respective receptors (GO:0005125, GO:0008009, GO:0004896, and GO:0004950, respectively), in AAMϕ-associated clusters were identified based on Gene Ontology annotations. Hierarchical clustering analysis reveals a unique expression profile of AAMϕ-associated immune effectors.

Cytokine and cytokine receptor expression profiles. Cytokine receptor expression was typically maintained or enhanced in NeMϕ. AAMϕ-up clusters contained the IL33 receptor *Il1rl1* (ST-2) and the IL27 receptor subunit *Il27ra* (WSX-1), both of which have previously been characterized as AAMϕ-associated.[21,22] AAMϕ-up clusters also included *Gfra2* (GDNF family receptor α-2), involved in neuronal survival and differentiation,[23] and the leptin receptor (*Lepr*). Leptin is an adipokine involved in energy homeostasis with broad, pleiotropic effects. There is no described role for leptin in Th2 immunity; however, macrophages of *Lepr*-deficient mice express higher levels of inflammatory cytokines,[24] suggesting the possibility that the leptin receptor contributes to the anti-inflammatory profile of AAMϕ.

With regard to cytokines, WT-NeMϕ produced significantly more *Il6*, *Wnt2*, and *Bmp6* than either WT-ThioMϕ or IL4Rα$^{-/-}$-NeMϕ. *Bmp6* is pleiotropic, suppressing B-cell proliferation[25] and promoting macrophage IL6 production.[26] *Wnt2* has no defined role in macrophage physiology, although Wnts do influence immune cell fate decisions.[27] Thus, *Wnt2* and *Bmp6* represent promising novel candidates for future investigations of Th2 immunity.

AAMϕ are described as broadly anti-inflammatory,[1] in part because of their production of IL10. Surprisingly, in the chronic setting of our experiment, WT-NeMϕ did not produce any IL10 (supplemental Table 5). Nonetheless, AAMϕ-down clusters contained many proinflammatory cytokines. Among these were *Tnf*, *Lif*, *Il1b*, and *Il16*.[28-30] In addition, the expression of the macrophage activating factor *Tnfsf9*[31] and the IL27 and IL35 subunit *Ebi3* were lowered in AAMϕ. In summary, AAMϕ expressed greater levels of immune effectors associated with eosinophil recruitment and survival and lower levels of numerous proinflammatory agents.

KEGG pathway analysis

To assess whether metabolic changes in macrophages previously observed during IL4 treatment in vitro also occur in vivo, we applied gene set enrichment analysis (GSEA) using the KEGG pathway database alongside modifications for RNA-Seq data (see supplemental Methods). By considering the relative expression of all genes, rather than only DE genes, GSEA provides a sensitive metric for identifying differences in biochemical and cell signaling pathways.

The complement and coagulation cascade. Unexpectedly, the complement and coagulation cascade (KEGG pathway mmu04610) was the most differentially regulated pathway between WT-NeMϕ and WT-ThioMϕ (supplemental Table 6). The most striking feature of complement expression in AAMϕ was transcript abundance (Figure 5). For example, *C3* and *C4* attracted > 100 000 reads each, making them among the most abundant NeMϕ-associated transcripts. NeMϕ showed up-regulation of C1q complex genes (*C1qa*, *C1qb*, and *C1qc*), and striking overexpression of MBL pathway constituents, specifically FicolinA (*FcnA*), *Cfb*, and *Cfp* (supplemental Figure 9). This suggests a role for FicolinA-dependent complement activity in the response to helminth infection.

Mitochondrial metabolism. Twenty-three of the 27 most differentially regulated pathways between WT-NeMϕ and WT-ThioMϕ were metabolic (supplemental Figure 10; supplemental Table 6). A similar trend was observed between WT-NeMϕ and IL4Rα$^{-/-}$-NeMϕ, supporting a model wherein a shift in metabolic phenotype is a cardinal feature of alternative activation[4] (supplemental Figure 10). The second most perturbed KEGG pathway between WT-NeMϕ and WT-ThioMϕ was the tricarboxylic acid (TCA) cycle (supplemental Table 6). Indeed, the majority of expressed TCA cycle genes were expressed at a higher level in WT-NeMϕ

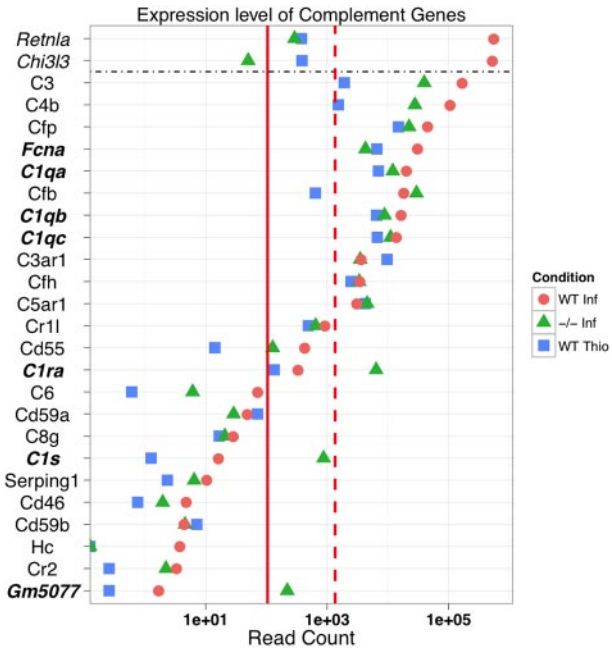

Figure 5. Complement components are abundantly expressed in an alternative activation-dependent manner. The expression of genes in the complement and coagulation cascade (KEGG pathway mmu:04610). For reference, the median and 90th percentiles of expression for all expressed genes are included (solid and dashed red lines, respectively). In addition, highly expressed marker genes *Chi3l3* (YM-1) and *Retnla* (RELMα) are included for reference.

relative to both WT-ThioMϕ and IL4Rα$^{-/-}$-NeMϕ (Figure 6A; supplemental Figure 11). A similar pattern of gene expression was also observed for genes involved in oxidative phosphorylation (Figure 6B). Taken together, these findings are consistent with previous studies showing that IL4 induces expansion of the mitochondrial compartment in macrophages in vitro.[32]

PPARγ and PGC-1β, key regulators of mitochondrial metabolism, have been described as required for alternative macrophage activation in vitro.[12,32] Accordingly, the metabolic profile we observe could be explained by transcriptional activity of PPAR family members (PPARα, PPARγ, and PPARδ). However, during *B malayi* infection, macrophage-specific PPARγ$^{-/-}$ mice show no impairment in alternative activation (D.R., unpublished data, October 2009). Furthermore, although PGC-1β expression was augmented in an IL4Rα- and infection-dependent manner, PPARγ levels were substantially lower in NeMϕ than ThioMϕ (Figure 6C). PPARα was not expressed by any of the assayed macrophage populations (supplemental Table 5). Only PPARδ expression was sustained in NeMϕ, yet it was not up-regulated (Figure 6C). This suggests that, during helminth infection, PPARδ may compensate, either partially, or completely, for reduced PPARγ in NeMϕ. Alternatively, PPAR-independent transcription may maintain mitochondrial metabolism in NeMϕ.

TSS identification and promoter region analysis

To address whether PPARs facilitate transcription of IL4Rα-dependent genes in vivo we analyzed transcription factor binding sites (TFBSs) in the promoters of AAMϕ-associated genes. We developed and optimized a method to accurately identify TSSs using RNA-Seq data (Figure 6D; for details of the method and validation, see supplemental Methods). Briefly, transcripts were defined using Cufflinks,[33] and TSSs identified based on expected gene expression and the observed sequencing read depth at each position in the gene. Proximal promoter sequences

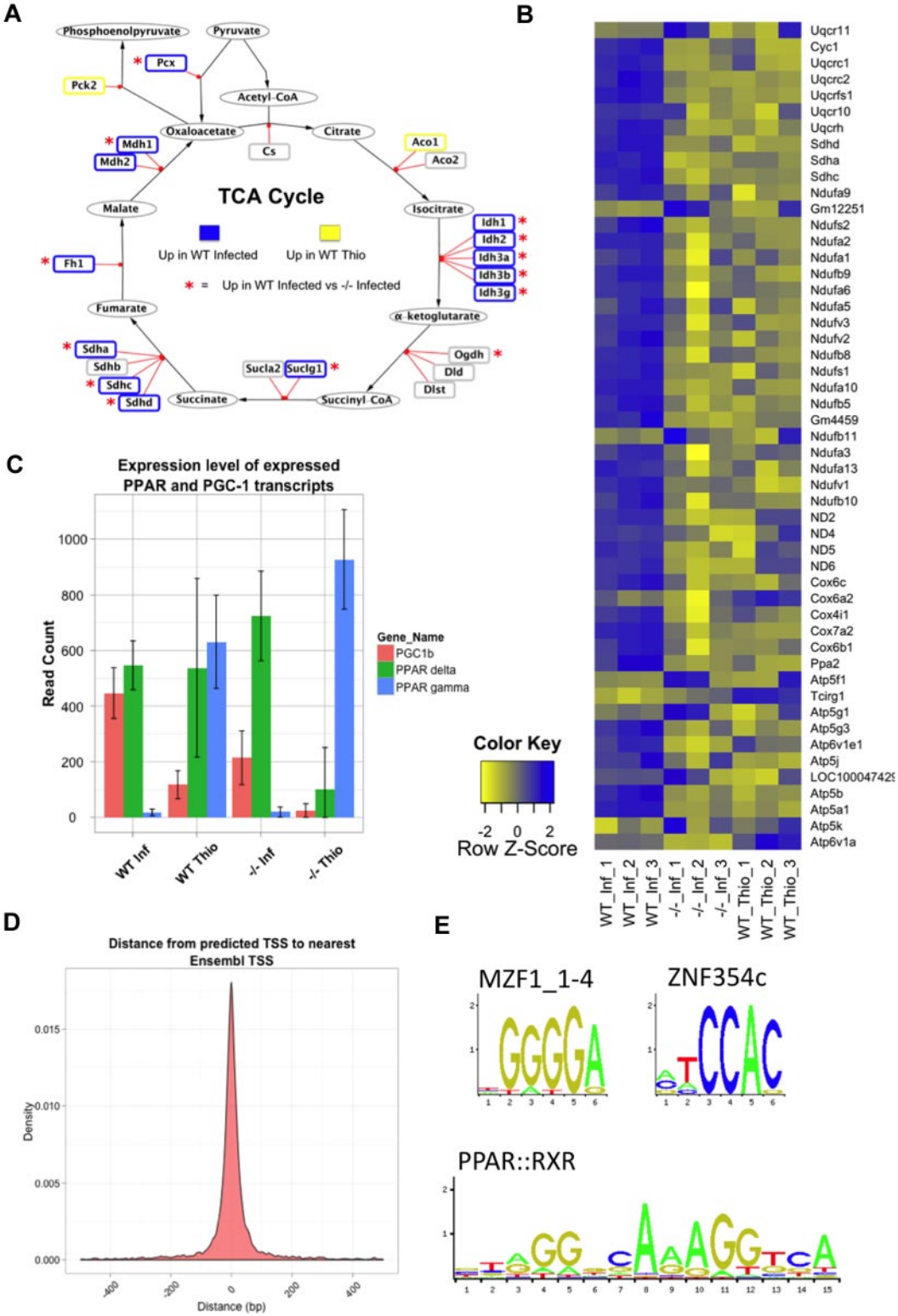

Figure 6. AAMϕ up-regulate mitochondrial TCA cycle genes and show evidence of PPAR-dependent transcription in vivo. (A) Schematic of the TCA cycle showing DE genes in WT-NeMϕ relative to WT-ThioMϕ. Blue border represents up-regulated; and yellow border, down-regulated. In addition, a red asterisk indicates genes up-regulated in WT-NeMϕ relative to IL4Rα$^{-/-}$-NeMϕ. (B) Heatmap showing relative expression of mitochondrial electron transport chain (ETC) components between WT-NeMϕ, IL4Rα$^{-/-}$-NeMϕ, and WT-ThioMϕ. The majority of ETC components are most highly expressed in WT-NeMϕ. (C) The expression levels of transcripts encoding for PPARγ, PPARδ, and the coactivator protein PGC-1β show that WT-NeMϕ express high levels of PPARδ and PGC-1β, but not PPARγ. (D) Confirmation of the accuracy of TSS prediction. The density plot shows the distances from the predicted TSS for each gene to the nearest annoated Ensembl TSS (median absolute deviation = 32 bp). (E) Consensus motifs for the 3 over-represented transcription factor binding sites in AAMϕ-associated promoter regions identified using Clover ($P < .01$), comparison of AAMϕ-associated promoter regions (TSS −400, +100 bp) against non-AAMϕ-associated macrophage promoters.

Table 2. The 3 statistically over-represented position weight matricies in AAMϕ-associated promoters relative to all macrophage promoters

Jaspar motif	Clover *P*
MZF1_1-4 zinc-coordinating	.000
PPARG::RXRA zinc-coordinating	.004
ZNF354C zinc-coordinating	.006

Clover *P* value was determined by permutation test with 1000 iterations.

(300 bp upstream and 100 bp downstream of each TSS) were obtained from 7817 high-confidence TSSs and analyzed for over-represented TFBSs.

We validated our method by identifying over-represented TFBSs in our promoters relative to all mouse promoters using Clover,[34] and comparing the found set with the macrophage lineage-restricted TFBSs identified by Hume et al.[35] In our data, we identified 54 motifs that were present significantly more often than expected ($P < .01$). Hume et al[35] used a different library of TFBS motifs and identified 27 significant motifs, 23 of which were represented in the library we used. Our analysis identified 18 of these (78%) as over-represented in our macrophage promoters, reinforcing the findings of the previous study and confirming the accuracy of our predictions.

Promoters were categorized according to the expression characteristics of their parent genes. We identified 682 AAMϕ-associated promoters, derived from genes up-regulated in WT-NeMϕ relative to both WT-ThioMϕ and IL4Rα$^{-/-}$-NeMϕ. The remaining 7135 promoters were classified as generic macrophage promoters. We compared AAMϕ-associated promoters to the generic set, and identified only 3 over-represented TFBS motifs: MZF1, ZNF354c, and PPARG:RXRA (also known as PPAR response element [PPRE]; Table 2; Figure 6E). We used the Regulatory Sequence Analysis Toolkit[36] to count the number of instances of each motif within our set of 682 AAMϕ-associated promoters and found that 113 (17%) contained high-confidence PPRE elements. Because the MZF1_1-4 and ZNF354c consensus motifs are very short, we could not quantify these at the default significance threshold ($P < .00001$). The observation of an abundant and over-represented PPRE identifies PPAR-mediated transcription as a significant component of AAMϕ-associated transcriptional regulation in vivo.

Analysis and quantification of NeMϕ-derived eicosanoids

GO and KEGG GSEA identified augmented mitochondrial and metabolic gene expression, specifically the TCA cycle, as infection and IL4Rα-dependent processes (Figure 6A-B). Our analysis of AAMϕ-associated *cis*-regulatory features further supported a role for PPAR involvement (Figure 6E). Together, these strongly suggest that PPAR-mediated transcription is a driving component of the AAMϕ phenotype in vivo. PPARγ and oxidative phosphorylation are described as necessary for alternative activation,[4] yet NeMϕ PPARγ expression was low (Figure 6C). As PPARδ potentiates alternative kupffer cell[37] and adipose tissue macrophage activation[38] we hypothesized that it may compensate for PPARγ in NeMϕ. The PPAR family are ligand-dependent transcription factors. Thus, although PPARδ was not DE, we explored the possibility that increased ligand availability might modulate PPARδ-dependent transcription in NeMϕ.

KEGG pathway analysis identified arachidonic acid (AA) metabolism, a known source of PPAR ligands, as up-regulated in WT-NeMϕ (supplemental Table 6). Products of the AA enzyme cascade, eicosanoids, compose a wide variety of proinflammatory and anti-inflammatory mediators, including the prostaglandins, leukotrienes, and lipoxins. We characterized a broad range of these compounds produced by NeMϕ and ThioMϕ using LC-MS/MS in an independent, homologous experiment (lacking the IL4Rα$^{-/-}$ thioglycollate group). Individual eicosanoids (for a full list of species, see supplemental Methods) were measured in peritoneal lavage fluid and ex vivo in 12-hour cultures of adherence-purified macrophages. Ex vivo cultures showed that NeMϕ produced significantly more eicosanoids than ThioMϕ (Figure 7A) irrespective of IL4Rα expression. This cannot be attributed to enhanced activity of the AA-liberating phospholipase A2 enzymes as Pla2 transcripts were expressed in ThioMϕ at a comparable level to NeMϕ (supplemental Figure 12). This suggests that IL4Rα-independent effects of *B malayi* drive AA catabolism.

Principal component analysis (PCA) of eicosanoid profiles from cultured macrophages showed that the 3 treatment groups formed distinct clusters (Figure 7B). IL4Rα$^{-/-}$-NeMϕ produced high levels of proinflammatory PGE_2 and downstream metabolites that promote acute phase inflammation.[39] WT-NeMϕ were characterized by production of the 12/15-lipoxygenase–derived HETE metabolites, predominantly 12-HETE (Figure 7C). Interestingly, by far the most abundant Cox derivative in WT-NeMϕ was 6-keto-$PGF_{1\alpha}$, the auto-oxidation product of the PPARδ agonist prostacyclin (PGI_2 [39]; Figure 7D).

Integrating the lipidomic profiles and gene expression data allowed us to better understand the relationship between transcriptional profiles and metabolic phenotype. We plotted gene expression and metabolite data onto a pathway map of the enzymatic cascade, relating AA catabolism to metabolite production.[41] Alterations in synthase gene expression showed high concordance with the relative abundances of daughter metabolites (Figure 7E), with one notable exception. Despite robust expression of *Gpx1*, *Alox5*, and *Lta4h*, we were unable to detect any 5-lipoxygenase derived metabolites, 5-HETE 5-OxoETE, LTB_4, or 20-OH LTB_4 (supplemental Figure 13). Thus peritoneal macrophages were primed to produce leukotrienes but did not. Substrate competition for AA or higher-level control of leukotriene biosynthesis may explain this observation. In summary, eicosanoid production by macrophages is stimulated in response to *B malayi*. Rather than affecting total eicosanoid production, IL4Rα-dependent signaling modulated the architecture of the downstream enzymatic cascade, leading to a more anti-inflammatory eicosanoid profile.

Heterotypic interactions contribute toward the eicosanoid profile in vivo. To discern the relative contributions of macrophage- and non–macrophage-derived eicosanoids, we measured AA products in peritoneal lavage from the mice in the same experiment (supplemental Figure 13). PCA plots (Figure 7F) showed no distinction between WT thioglycollate-injected and IL4Rα$^{-/-}$-*B malayi*–implanted mice. The WT *B malayi*–implanted individuals, however, clustered distinctly, showing that the response to *B malayi* implantation generated a unique, IL4Rα-dependent, eicosanoid environment. This also implies that *B malayi* is not a major source of total peritoneal eicosanoids in this model. WT-implanted mice had increased HETE, PGD_2, and TxB_2 concentrations (Figure 7G), the latter 2 of which are eosinophil chemoattractants.[42,43] It is unlikely that the PGD_2 was macrophage-derived as low levels were produced in AAMϕ ex vivo cultures. TxB_2 concentrations correlated with, and may be explained by, the increase in macrophage numbers associated with infection in a WT environment (supplemental Figure 14A-B). We have therefore identified a distinct lipid effector profile in the response to helminth infection. Although the activity of 5-lipoxygenase did not contribute toward this profile, the actions of cyclooxygenase and 12/15-lipoxygenase did.

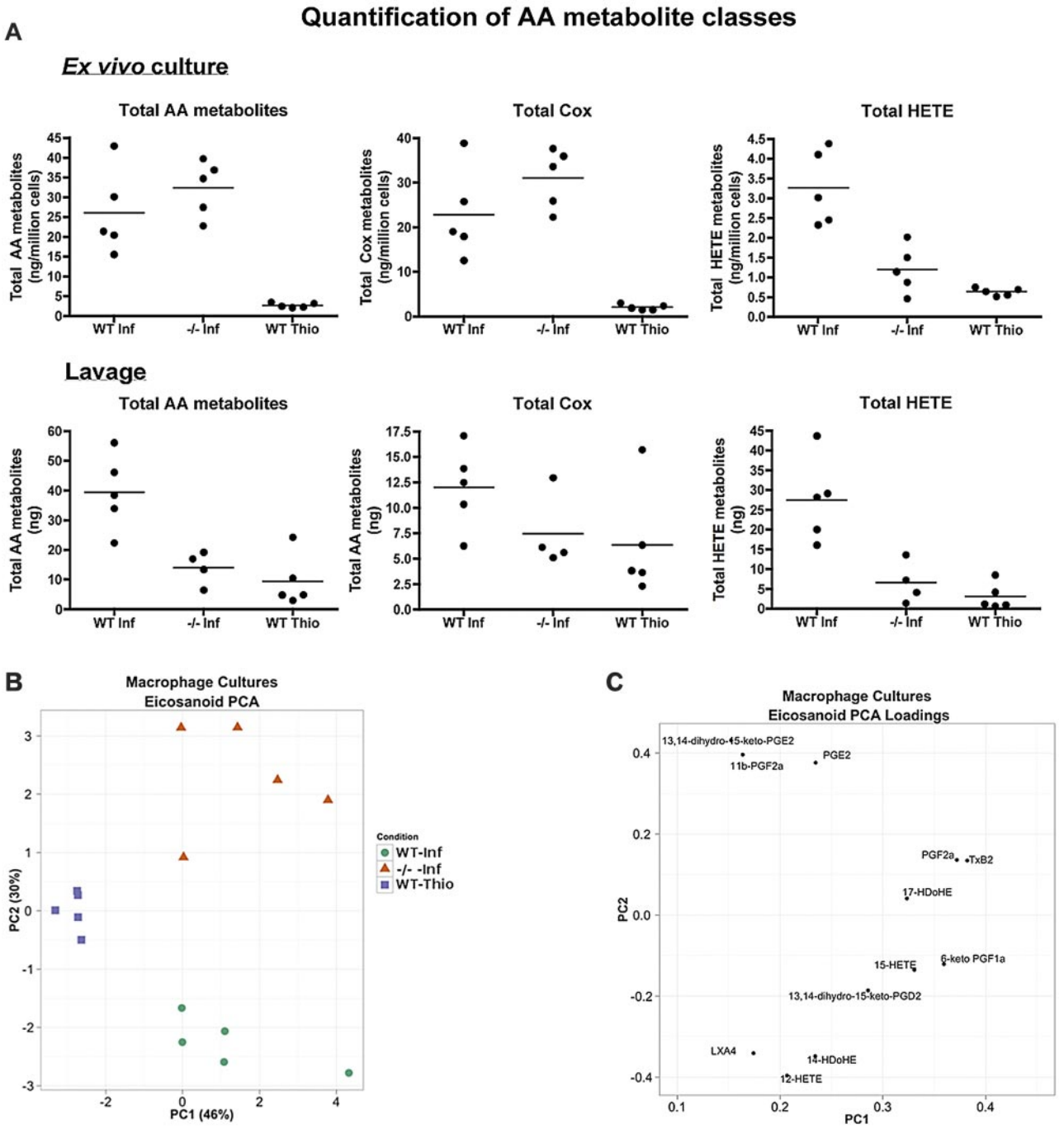

Figure 7. Characterization of AAMϕ-derived eicosanoids. (A) Quantification of arachidonic acid (AA) metabolites in 12-hour cultures of purified macrophages (top) and in peritoneal lavages (bottom). (B) PCA scores plot for 12-hour cultures of purified macrophages. (C) PCA loading plot for panel B, showing how individual eicosanoids contribute toward the primary and secondary principal (x and y, respectively) axes. (Figure continues on next page.)

Discussion

We have characterized the phenotype of *B malayi*–elicited AAMϕ using RNA-Seq and a targeted lipid analysis. Together, these reveal the effects of IL4Rα-dependent signaling on macrophage physiology in a chronic Th2 environment. Our findings strongly support the emerging paradigm that alternative activation and inflammation are associated with wholesale alterations in metabolism.[4] Further, GSEA and a detailed analysis of AAMϕ-associated chemokine and cytokine expression provide intriguing clues as to the physiologic role(s) of AAMϕ in vivo.

One of the more unexpected findings of our analysis was that, collectively, macrophage complement genes were among the most abundantly expressed and differentially regulated in the response to helminth challenge and may represent a previously unrecognized effector axis of AAMϕ. A requirement for complement in antihelminthic immunity has previously been demonstrated, as C3 mediates clearance during both *Strongyloides stercorallis*[44] and *Schistosoma mansoni* infection.[45] In the context of *B malayi*, complement

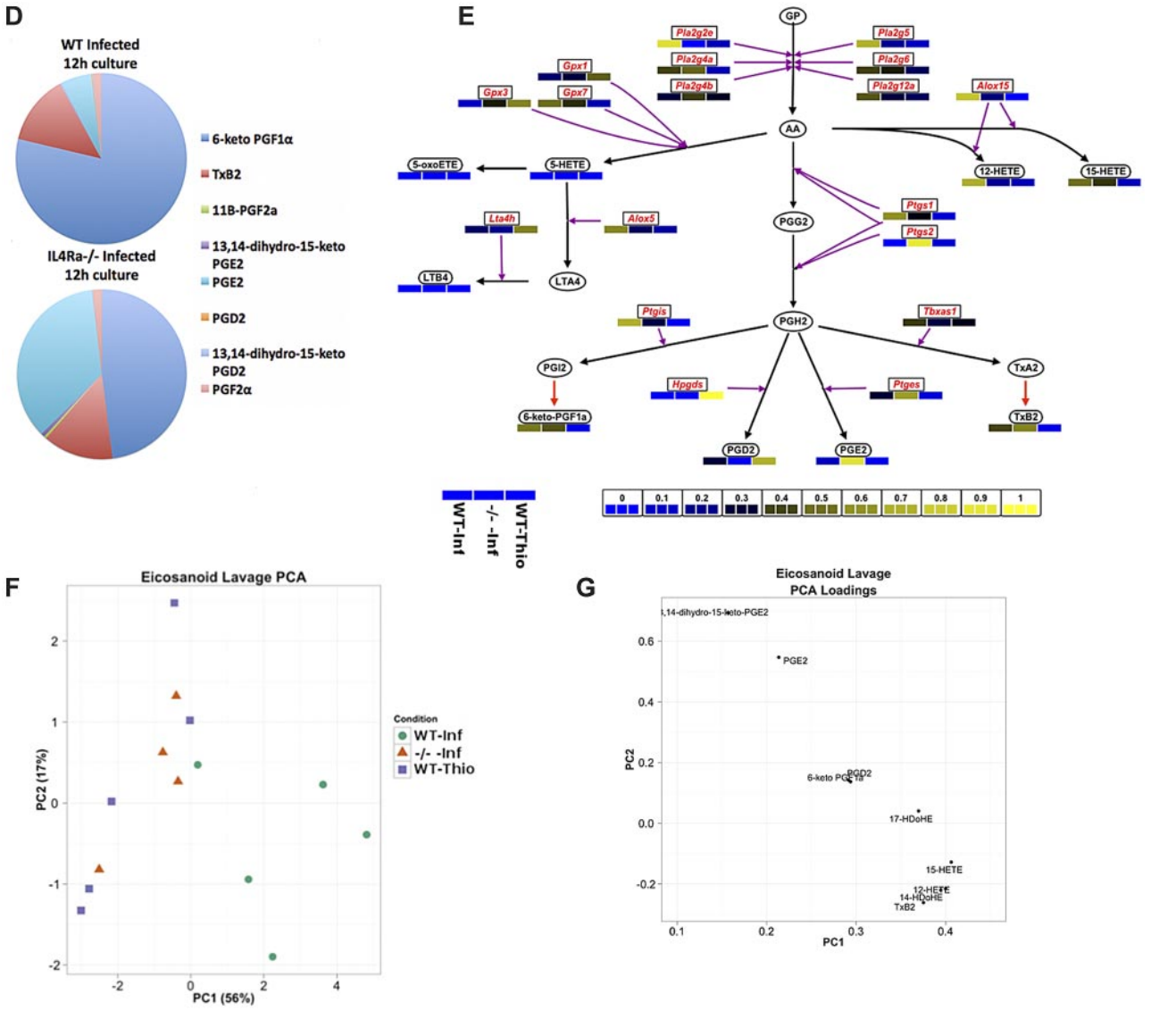

Figure 7. (continued) (D) Pie chart showing the breakdown in the production of cyclo-oxygenase metabolites between WT-NeMϕ and IL4Rα$^{-/-}$-NeMϕ. (E) Schematic of the AA cascade reproduced using VANTED. Square boxes with red text represent genes; and rounded boxes with black text, measured metabolites. Black arrows indicate enzymatic reactions; and red arrows, auto-oxidation. Relative expression values (normalized such that the total over all 3 conditions = 1) are beneath the associated gene/metabolite. WT *B malayi* (left box) IL4Rα$^{-/-}$ *B malayi* implanted (center), and WT thioglycollate (right). (F-G) PCA scores and loading plot as in panels B and C for the peritoneal lavages.

interacts with microfilariae[46] and may contribute toward their clearance. Here we identify AAMϕ-derived *Fcna* as a candidate for further study into the regulation of the complement response to filarial nematode infection.

We also identified IL4Rα-dependent expression of cytokines not currently associated with AAMϕ physiology, including *Bmp6* and *Wnt2*. Intriguingly, Bmp6 has been associated with increased macrophage iNOS activity, suggesting that it may curtail alternative activation.[47] *Wnt2* is a highly abundant AAMϕ-derived cytokine with no identified role in macrophage biology. *Wnt2* does, however, affect hematopoietic lineage commitment,[48] and our AAMϕ-up clusters contained *Cdh1* (E-cadherin), an AAMϕ marker in both humans and mice.[49] Given the known convergence between cadherin and Wnt pathways, further work to elucidate the role of *Wnt2* in macrophage biology is warranted. We have observed IL4Rα and infection-dependent production of cytokines, chemokines, and eicosanoids, suggesting that NeMϕ aid in the orchestration and maintenance of the immune environment. Specifically, NeMϕ potentially regulate eosinophil recruitment via multiple, redundant, mechanisms. Reese et al previously demonstrated chitin-induced eosinophilia as an AAMϕ-dependent process,[50] but whether they fulfill this role in the more complex environment of live parasite infection is unclear. We show here that WT-NeMϕ transcribe eosinophil chemotactic factors in vivo. *Ccl8*[16] and *Ccl24*[17] operate as *Ccr3* ligands, whereas TxA_2,[43] the bioactive precursor of TxB_2, induces eosinophilia by affecting vascular epithelial integrin expression. Our data are therefore consistent with AAMϕ-mediated recruitment and maintenance of eosinophilia during helminth infection. Interestingly, in contrast to the work by Reese et al,[50] our proposed mechanism for eosinophil recruitment is LTB_4-independent. Our findings may differ because Reese et al used an acute stimulus, whereas we use a chronic model of helminth infection. Nevertheless, our data suggest cooperative interactions between AAMϕ-derived protein and lipid mediators ensure robust, tightly regulated eosinophil recruitment to sites of infection.

IL4Rα-dependent signaling led to reduced expression of multiple proinflammatory cytokines and chemokines, supporting a

model wherein AAMϕ are anti-inflammatory or noninflammatory. Macrophage PPAR activity augments alternative activation and reduces the expression of proinflammatory cytokines.[4] Indeed, thiazolidenediones, antidiabetic PPARγ agonists, improve insulin sensitivity in obese white adipose tissue (WAT) partly by curtailing CAMϕ.[4] Global similarities can be drawn between our surveyed NeMϕ and the beneficial AAMϕ in WAT of lean individuals, including enhanced oxidative metabolism and low proinflammatory cytokine expression.[4] By assaying TFBS in NeMϕ promoters, we provide compelling evidence that PPAR-mediated transcription is an important facet of the macrophage response to helminth infection in vivo. WAT AAMϕ and NeMϕ are however distinct subsets. WAT AAMϕ express PPARγ, *Il10*, and *Cd36*,[51] whereas *Cd36* and PPARγ were down-regulated, and *Il10* was not expressed, in NeMϕ (supplemental Table 3). This is consistent with alveolar AAMϕ failing to express IL10 in response to *Nippostrongylus brasiliensis*.[52] However, the observation that *N brasiliensis*–infected mice show improved glucose tolerance[53] demonstrates that the physiologic consequences of modulating alternative activation, either in the response to infectious disease or during homeostasis, imparts similarities that are greater than the observed differences between WAT AAMϕ and NeMϕ. This is perhaps not surprising as alternative activation in both these disparate environments is STAT6-dependent. An improved understanding of the influence of context-specific (ie, tissue/infection model) cues in fine-tuning AAMϕ polarization is required to fully appreciate the functional diversity of AAMϕ phenotypes.

We observed low PPARγ expression in NeMϕ, consistent with a recent report of PPARγ expression profiles in different macrophage subsets.[54] Analysis of AAMϕ-associated *cis*-regulatory regions suggested a role for PPARs in WT-NeMϕ, and we therefore sought a mechanism for PPAR-dependent transcription during *B malayi* infection. By profiling macrophage-derived eicosanoids, we found that nematode-, but not thioglycollate-elicited, macrophages abundantly produced the PPARδ ligand PGI_2. Because of the low expression of PPARγ in NeMϕ and constitutive PPARδ expression, macrophage PGI_2 production provides a feasible and testable explanation for the maintenance of PPAR-dependent transcription in NeMϕ. However, it should be noted that, because NeMϕ do express PPARγ, we cannot rule out a role for both these transcription factors during alternative activation. We have shown that macrophage eicosanoid generation is IL4Rα independent in this system. This suggests that the liberation of PPAR ligands is *B malayi*–mediated and is perhaps achieved via a pathogen associated molecular pattern-dependent mechanism. IL4Rα-dependent signaling did, however, alter the expression of AA catabolic enzymes, enhancing the production of anti-inflammatory HETEs.[3] Hence, extracellular cues (ie, IL4/IL13) manipulated the architecture of the enzymatic cascade, reorganizing the eicosanoid landscape. Ultimately, this reduced proinflammatory eicosanoid production and increased the synthesis PGI_2 and anti-inflammatory HETEs. We propose a model in which the presence of a "danger signal" is coupled with cytokine-dependent structural reorganization, providing both an initiator and higher-order specificity that contributes toward sustaining the NeMϕ phenotype in vivo.

We have defined the phenotype of IL4Rα-stimulated AAMϕ in vivo during the response to a nematode infection. All of the data we present are supportive of anti-inflammatory roles for AAMϕ in this setting. To summarize, WT-NeMϕ broadly down-regulated the expression of numerous proinflammatory cytokines and chemokines. The eicosanoid environment generated by NeMϕ is defined by enhanced production of anti-inflammatory HETE metabolites and also the abundant production of the PPARδ ligand PGI_2. We infer that NeMϕ have a decreased migratory capacity because of the down-regulation of multiple chemokines and therefore are unlikely to prime lymphatic T-cell responses. Our study has also identified the production of complement as a major component of the macrophage response to filarial nematode challenge. Although complement may aid in the recognition and clearance of either adult *B malayi* or microfilarae, it also has extensive immunoregulatory functions.[55] For example, complement C5a interacts with surface Fc receptors to modulate inflammation.[55] In this context, our WT-NeMϕ strongly up-regulated expression of the regulatory *Fcgr2b* (supplemental Table 3). Thus, the complement-Fc receptor axis induced by AAMϕ in the response to nematode challenge may be an additional anti-inflammatory feature of IL4Rα-dependent macrophage activation.

Acknowledgments

The authors thank Marian Thomson in the GenePool Genomics facility for support in RNA-Seq data generation, Martin Waterfall for expertise with flow sorting, and Tom Freeman, David Hume, Stephen Jenkins, and Lucy Jones for critical reading of the manuscript.

This work was supported by the Wellcome Trust (PhD studentship award, G.D.T.) and the MRC (program grant MRC-UK G0600818, J.E.A.; and core funding to the GenePool facility MRC 60900740, M.L.B.). B.H.M. and P.D.W were supported by the European Regional Development Fund, Highlands and Islands Enterprise, and the Scottish Funding Council.

Authorship

Contribution: G.D.T., D.R., M.L.B., and J.E.A. devised experiments; G.D.T. performed most of the experimental work and analyses; B.H.M., P.D.W., and G.D.T. performed lipidomics; G.D.T., M.L.B., and J.E.A. wrote the manuscript; and all authors contributed to writing the manuscript.

Conflict-of-interest disclosure: The authors declare no competing financial interests.

Correspondence: Mark L. Blaxter, Institute of Evolutionary Biology, School of Biological Sciences, University of Edinburgh, Edinburgh, EH9 3JT, United Kingdom; e-mail: mark.blaxter@ed.ac.uk; and Judith E. Allen, Institute of Immunology and Infection Research, School of Biological Sciences, University of Edinburgh, Edinburgh, EH9 3JT, United Kingdom; e-mail: j.allen@ed.ac.uk.

References

1. Gordon S, Martinez FO. Alternative activation of macrophages: mechanism and functions. *Immunity.* 2010;32(5):593-604.
2. Mantovani A, Sozzani S, Locati M, Allavena P, Sica A. Macrophage polarization: tumor-associated macrophages as a paradigm for polarized m2 mononuclear phagocytes. *Trends Immunol.* 2002;23(11):549-555.
3. Allen JE, Maizels RM. Diversity and dialogue in immunity to helminths. *Nat Rev Immunol.* 2011; 11(6):375-388.
4. Odegaard JI, Chawla A. Alternative macrophage activation and metabolism. *Annu Rev Pathol.* 2011;6:275-297.
5. Jenkins SJ, Ruckerl D, Cook PC, et al. Local macrophage proliferation, rather than recruitment from the blood, is a signature of Th2 inflammation. *Science.* 2011;332(6035):1284-1288.

6. Hashimoto D, Miller J, Merad M. Dendritic cell and macrophage heterogeneity in vivo. *Immunity.* 2011;35(3):323-335.
7. Loke P, Nair M, Parkinson J, et al. Il-4 dependent alternatively-activated macrophages have a distinctive in vivo gene expression phenotype. *BMC Immunol.* 2002;3(1):7.
8. van der Windt GJW, Everts B, Chang C-H, et al. Mitochondrial respiratory capacity is a critical regulator of CD8+ T cell memory development. *Immunity.* 2012;36(1):68-78.
9. Infantino V, Convertini P, Cucci L, et al. The mitochondrial citrate carrier: a new player in inflammation. *Biochem J.* 2011;438(3):433-436.
10. Rodríguez-Prados J-C, Través PG, Cuenca J, et al. Substrate fate in activated macrophages: a comparison between innate, classic, and alternative activation. *J Immunol.* 2010;185(1):605-614.
11. Szanto A, Balint BL, Nagy ZS, et al. Stat6 transcription factor is a facilitator of the nuclear receptor PPARγ-regulated gene expression in macrophages and dendritic cells. *Immunity.* 2010;33(5):699-712.
12. Vats D, Mukundan L, Odegaard JI, et al. Oxidative metabolism and PGC-1beta attenuate macrophage-mediated inflammation. *Cell Metab.* 2006;4(1):13-24.
13. Sandler NG, Mentink-Kane MM, Cheever AW, Wynn TA. Global gene expression profiles during acute pathogen-induced pulmonary inflammation reveal divergent roles for Th1 and Th2 responses in tissue repair. *J Immunol.* 2003;171(7):3655-3667.
14. Trapnell C, Pachter L, Salzberg SL. Tophat: discovering splice junctions with RNA-Seq. *Bioinformatics.* 2009;25(9):1105-1111.
15. Loke P, Gallagher I, Nair MG, et al. Alternative activation is an innate response to injury that requires CD4+ T cells to be sustained during chronic infection. *J Immunol.* 2007;179(6):3926-3936.
16. Romagnani S. Cytokines and chemoattractants in allergic inflammation. *Mol Immunol.* 2002;38(12-13):881-885.
17. Mantovani A, Sica A, Sozzani S, et al. The chemokine system in diverse forms of macrophage activation and polarization. *Trends Immunol.* 2004;25(12):677-686.
18. Sánchez-Martín L, Estecha A, Samaniego R, et al. The chemokine CXCL12 regulates monocyte-macrophage differentiation and RUNX3 expression. *Blood.* 2011;117(1):88-97.
19. Mylonas KJ, Nair MG, Prieto-Lafuente L, Paape D, Allen JE. Alternatively activated macrophages elicited by helminth infection can be reprogrammed to enable microbial killing. *J. Immunol.* 2009;182(5):3084-3094.
20. Loke P, MacDonald AS, Allen JE. Antigen-presenting cells recruited by Brugia malayi induce Th2 differentiation of naive CD4(+) T cells. *Eur J Immunol.* 2000;30(4):1127-1135.
21. Kurowska-Stolarska M, Stolarski B, Kewin P, et al. IL33 amplifies the polarization of alternatively activated macrophages that contribute to airway inflammation. *J Immunol.* 2009;183(10):6469-6477.
22. Rückerl D, Hessmann M, Yoshimoto T, Ehlers S, Hölscher C. Alternatively activated macrophages express the il-27 receptor alpha chain wsx-1. *Immunobiology.* 2006;211(6-8):427-436.
23. Jing S, Yu Y, Fang M, et al. GFRalpha-2 and GFRα-3 are two new receptors for ligands of the GDNF family. *J Biol Chem.* 1997;272(52):33111-33117.
24. Li S, Reddy MA, Cai Q, et al. Enhanced proatherogenic responses in macrophages and vascular smooth muscle cells derived from diabetic db/db mice. *Diabetes.* 2006;55(9):2611-2619.
25. Kersten C, Sivertsen EA, Hystad ME, et al. BMP-6 inhibits growth of mature human B cells: induction of Smad phosphorylation and upregulation of Id1. *BMC Immunol.* 2005;6:9.
26. Lee GT, Kwon SJ, Lee J-H, et al. Induction of interleukin-6 expression by bone morphogenetic protein-6 in macrophages requires both Smad and p38 signaling pathways. *J Biol Chem.* 2010;285(50):39401-39408.
27. Staal FJT, Luis TC, Tiemessen MM. WNT signalling in the immune system: WNT is spreading its wings. *Nat Rev Immunol.* 2008;8(8):581-593.
28. de Rosado JD, Rodriguez-Sosa M. Macrophage migration inhibitory factor (MIF): a key player in protozoan infections. *Int J Biol Sci.* 2011;7(9):1239-1256.
29. Tofaris GK, Patterson PH, Jessen KR, Mirsky R. Denervated schwann cells attract macrophages by secretion of leukemia inhibitory factor (LIF) and monocyte chemoattractant protein-1 in a process regulated by interleukin-6 and LIF. *J Neurosci.* 2002;22(15):6696-6703.
30. Cruikshank WW, Kornfeld H, Center DM. Interleukin-16. *J Leukoc Biol.* 2000;67(6):757-766.
31. Kim D-K, Lee SC, Lee H-W. CD137 ligand-mediated reverse signals increase cell viability and cytokine expression in murine myeloid cells: involvement of MTOR/p70s6 kinase and Akt. *Eur J Immunol.* 2009;39(9):2617-2628.
32. Odegaard JI, Ricardo-Gonzalez RR, Goforth MH, et al. Macrophage-specific PPARgamma controls alternative activation and improves insulin resistance. *Nature.* 2007;447(7148):1116-1120.
33. Trapnell C, Williams BA, Pertea G, et al. Transcript assembly and quantification by RNA-Seq reveals unannotated transcripts and isoform switching during cell differentiation. *Nat Biotechnol.* 2010;28(5):511-515.
34. Frith MC, Fu Y, Yu L, et al. Detection of functional DNA motifs via statistical over-representation. *Nucleic Acids Res.* 2004;32(4):1372-1381.
35. Hume DA, Summers KM, Raza S, Baillie JK, Freeman TC. Functional clustering and lineage markers: insights into cellular differentiation and gene function from large-scale microarray studies of purified primary cell populations. *Genomics.* 2010;95(6):328-338.
36. Thomas-Chollier M, Defrance M, Medina-Rivera A, et al. RSAT 2011: regulatory sequence analysis tools. *Nucleic Acids Res.* 2011;39(Web Server issue):W86-W91.
37. Odegaard JI, Ricardo-Gonzalez RR, Red Eagle A, et al. Alternative m2 activation of kupffer cells by ppardelta ameliorates obesity-induced insulin resistance. *Cell Metab.* 2008;7(6):496-507.
38. Kang K, Reilly SM, Karabacek V, et al. Adipocyte-derived th2 cytokines and myeloid ppardelta regulate macrophage polarization and insulin sensitivity. *Cell Metab.* 2008;7(6):485-495.
39. Trebino CE, Stock JL, Gibbons CP, et al Impaired inflammatory and pain responses in mice lacking an inducible prostaglandin E synthase. *Proc Natl Acad Sci U S A.* 2003;100(15):9044-9049.
40. Lim H, Dey SK. Minireview. A novel pathway of prostacyclin signaling: hanging out with nuclear receptors. *Endocrinology.* 2002;143(9):3207-3210.
41. Dennis EA, Deems RA, Harkewicz R, et al. A mouse macrophage lipidome. *J Biol Chem.* 2010;285(51):39976-39985.
42. Arima M, Fukuda T. Prostaglandin D2 and T(H)2 inflammation in the pathogenesis of bronchial asthma. *Korean J Intern Med.* 2011;26(2):253.
43. Ishizuka T, Kawakami M, Hidaka T, et al. Stimulation with thromboxane A2 (TXA2) receptor agonist enhances ICAM-1, VCAM-1 or ELAM-1 expression by human vascular endothelial cells. *Clin Exp Immunol.* 1998;112(3):464-470.
44. Kerepesi LA, Hess JA, Nolan TJ, Schad GA, Abraham D. Complement component C3 is required for protective innate and adaptive immunity to larval Strongyloides stercoralis in mice. *J Immunol.* 2006;176(7):4315-4322.
45. La Flamme AC, MacDonald AS, Huxtable CR, Carroll M, Pearce EJ. Lack of C3 affects TH2 response development and the sequelae of chemotherapy in schistosomiasis. *J Immunol.* 2003;170(1):470-476.
46. Carter T, Sumiya M, Reilly K, et al. Mannose-binding lectin A-deficient mice have abrogated antigen-specific IGM responses and increased susceptibility to a nematode infection. *J Immunol.* 2007;178(8):5116-5123.
47. Hong JH, Lee GT, Lee JH, et al. Effect of bone morphogenetic protein-6 on macrophages. *Immunology.* 2009;128(1 Suppl):e442-e450.
48. Wang H, Gilner JB, Bautch VL, et al. Wnt2 coordinates the commitment of mesoderm to hematopoietic, endothelial, and cardiac lineages in embryoid bodies. *J Biol Chem.* 2007;282(1):782-791.
49. Van den Bossche J, Bogaert P, van Hengel J, et al. Alternatively activated macrophages engage in homotypic and heterotypic interactions through IL4 and polyamine-induced E-cadherin/catenin complexes. *Blood.* 2009;114(21):4664-4674.
50. Reese TA, Liang H-E, Tager AM, et al. Chitin induces accumulation in tissue of innate immune cells associated with allergy. *Nature.* 2007;447(7140):92-96.
51. Liang C-P, Han S, Okamoto H, et al. Increased CD36 protein as a response to defective insulin signaling in macrophages. *J Clin Invest.* 2004;113(5):764-773.
52. Chen F, Liu Z, Wu W, et al. An essential role for T(H)2-type responses in limiting acute tissue damage during experimental helminth infection. *Nat Med.* 2012;18(2):260-266.
53. Shapiro H, Lutaty A, Ariel A. Macrophages, meta-inflammation, and immuno-metabolism. *Sci World J.* 2011;11:2509-2529.
54. Gautier EL, Chow A, Spanbroek R, et al. Systemic analysis of PPARgamma in mouse macrophage populations reveals marked diversity in expression with critical roles in resolution of inflammation and airway immunity. *J Immunol.* 2012;189(5):2614-2624.
55. Schmidt RE, Gessner JE. Fc receptors and their interaction with complement in autoimmunity. *Immunol Lett.* 2005;100(1):56-67.